Dynamic Response of Rubberized Concrete Columns with and without FRP Confinement Subjected to Lateral Impact

Thong M. Pham[1], X. Zhang[2], M. Elchalakani[3], A. Karrech[4], Hong Hao[5]* and Aarin Ryan[6]

Abstract

This study experimentally investigates the impact response of rubberized concrete columns subjected to lateral impact. A pendulum impact testing apparatus was used to test the concrete columns with varied rubber contents including 0%, 15%, and 30%. Fine and coarse aggregates were replaced by crumb rubber with particle sizes of 2-5 mm and 5-7 mm, respectively. The experimental results have shown that the rubberized concrete columns significantly reduce the peak impact force (27% - 40%) and thus mitigate the risk of injury and even death if rubberized concrete is used in roadside barriers. In addition, the rubberized concrete columns were more flexible than the normal concrete columns. They could deflect twice the reference columns before failure. Rubberized concrete significantly increased the impact energy absorption. The columns with 15% and 30% crumb rubber showed an increase in the impact energy absorption by 58% and 63% as compared to the reference columns. The rubberized concrete column confined with FRP outperformed the reference columns in terms of both the energy absorption

[1] Research Fellow, Center for Infrastructural Monitoring and Protection, School of Civil and Mechanical Engineering, Curtin University, Kent Street, Bentley, WA 6102, Australia. Email: thong.pham@curtin.edu.au
[2] Research Fellow, Center for Infrastructural Monitoring and Protection, School of Civil and Mechanical Engineering, Curtin University, Kent Street, Bentley, WA 6102, Australia. Email: xihong.zhang@curtin.edu.au
[3]Senior Lecturer, School of Civil, Environmental and Mining Engineering, the University of Western Australia, 35 Stirling Highway, WA 6009, Australia. Email: mohamed.elchalakani@uwa.edu.au
[4] Associate Professor, School of Civil, Environmental and Mining Engineering, the University of Western Australia, 35 Stirling Highway, WA 6009, Australia. Email: ali.karrech@uwa.edu.au
[5*]John Curtin Distinguished Professor, Center for Infrastructural Monitoring and Protection, School of Civil and Mechanical Engineering, Curtin University, Kent Street, Bentley, WA 6102, Australia, and School of Civil Engineering, Guangzhou University, Guangzhou 510006, China. Corresponding author's email: hong.hao@curtin.edu.au
[6]Former student, School of Civil, Environmental and Mining Engineering, the University of Western Australia, 35 Stirling Highway, WA 6009, Australia. Email: 21115408@student.uwa.edu.au

and load carrying capacity. Therefore, rubberized concrete is a better alternative and recommended for the use in roadside barriers to achieve better impact energy absorption capacity and reduce the maximum impact force under vehicle collisions.

Keywords: Rubberized concrete; Impact loading; Energy absorption; Roadside barriers.

Introduction

Used tires are among the largest and most problematic sources of waste in modern societies due to their durability. Millions of used tires are being discarded every year, which contain a number of environmentally damaging constituents, while only a small portion goes through recycling processes [1]. Tires typically require huge dumpsites as more than 75% of a tire volume are void. Furthermore, dumps can be turned into fertile grounds for proliferation of insects and on top of this microorganisms may also take more than 100 years to biodegrade the tires [1]. Therefore, it is necessary to find alternative solutions to recycle used tires and turn them into useful products.

Crumb rubber produced from used tires have been successfully utilized to replace aggregates in order to create new concrete, namely rubberized concrete [2-5]. Previous studies have shown that partially using rubber as aggregates in concrete increases its ductility, toughness, energy absorption, and damping ratio [1, 6-8]. However, previous studies also concluded that replacing normal aggregates by rubber reduces the structural strength properties of rubberized concrete [1, 9-11]. The reduction in these properties depends on many factors, such as the replacement of fine and/or coarse aggregates, the percentage of rubber replacement, and the use of any supplementary cementitious material such as silica fume. Elchalakani [1] recommended adding silica fume to the mix to improve the mechanical properties of rubberized concrete including the axial compressive strength, the flexural strength, and the modulus of elasticity. The author suggested that silica fume has enhanced the bonding at the interfacial transition zone so that it is beneficial to rubberized concrete.

Previous studies have shown that rubberized concrete can absorb more energy than conventional concrete [6, 7, 12]. The high energy absorption capacity of rubberized concrete can be utilized in structures where the energy absorption capacity is required rather than high

strength, for example, roadside barriers [1, 3, 6] and pedestrian pathways [13]. The impact resistance, defined as the combination of strength and dynamic energy absorption [14], was examined in previous studies on rubberized concrete [3, 8, 11, 15-17]. The impact resistance can be studied by well-established impact tests that are the weighted pendulum, Charpy-type impact, drop-weight, constant strain-rate test, projectile impact, split Hopkinson pressure bar, explosive test, and instrumented pendulum impact [14]. Most of the studies in the open literature examine the impact resistance of rubberized concrete by using simple drop-weight tests according to ACI 544.2R-17 [14]. The simplest and common method of the above impact tests is the repeated drop-weight impact test. The testing apparatus includes a 4.54 kg steel ball dropping from 0.45 m height. The steel ball is dropped multiple times on a specimen until the occurrence of the first crack and the ultimate failure. The energy absorption is measured from this type of impact test but not the strength. However, results of this type of impact tests are very scattered as mentioned by ACI 544.2R-17 [14]. There are studies in the literature investigating the axial impact resistance capacity of rubberized concrete [8, 15-17], however, no studies examined rubberized concrete columns against lateral impact. In addition, as rubberized concrete is utilized in roadside barriers, the lateral impact response of the structures become crucial to understanding the behaviour of roadside barriers under vehicle collisions while the axial impact resistance is relatively less relevant in this circumstance.

Beside unconfined rubberized concrete, Youssf et al. [18] investigated the structural behaviour of confined rubberized concrete columns under lateral cyclic loads. The authors concluded that using confined rubberized concrete slightly increased the peak strength and slightly decreased the ultimate drift compared to those of unconfined rubberized concrete. Meanwhile, the rubber particle sizes were found to have an insignificant effect on the energy dissipation and viscous damping of rubberized concrete. Xue and Shinozuka [19] conducted shaking table tests on rubberized concrete columns. The authors found that the damping coefficient of the rubberized

concrete columns increases by 62% as compared to normal concrete. In addition, the seismic response acceleration of rubberized concrete decreases by 27% as compared to normal concrete. Sukontasukkul et al. [20] recommended using rubberized concrete as a cushion layer in bulletproof concrete panels. The authors combined a soft rubberized concrete layer and a hard layer of steel fiber reinforced concrete to resist impact loads. The soft layer of rubberized concrete was designed to absorb energy and then transfer less impact energy to the hard layer. In another application, the impact response of real scale roadside barriers made of rubberized concrete was investigated by Atahan and Sevim [6]. The safety barriers had the height, base width, top width, and length of 1 m, 0.45 m, 0.25 m and 1 m, respectively. The authors used a 4-wheel vehicle with the weight of 500 kg for the impact tests and concluded that the energy absorption increased with the rubber content. Besides, rubberized concrete has another advantage of significantly reducing acceleration induced by an impact event thus mitigated injury risk to human occupants. The above studies have made a consensus that rubberized concrete yields higher energy absorption but lower strength than the corresponding conventional concrete. To propose rubberized concrete with higher energy absorption as well as higher strength, FRP confinement can be used since this technique has shown a significant increase in strength and energy absorption of conventional concrete under impact loads [21-23].

As far as the authors are aware, no study has been carried out to investigate the impact response of rubberized concrete columns under lateral impact. Since understanding the performances of the column subjected to lateral impact loads is essential for application of the column in roadside barrier constructions, pendulum impact tests were performed to investigate the impact response of rubberized concrete columns in this study. In total, 7 rubberized concrete columns were cast and tested with 800 mm height and 100 mm square section. Two different rubber contents including 15% and 30% were examined. A steel impactor weighing 300 kg was lifted

to certain heights before releasing to generate the impact loading on the mid-height of the columns. The progressive damage, the impact force time histories, the displacement time histories, and energy absorption capacity were examined and discussed.

Experimental program

In this study, seven reinforced rubberized concrete columns were cast and tested at the concrete laboratory of the University of Western Australia. Six columns were made of unconfined rubberized concrete and one column (15% rubber content) was wrapped with one layer of FRP. Among the six columns associated with unconfined rubberized concrete, there were three pairs including two columns with normal concrete (0% rubber), two columns with 15% rubberized concrete and the other two columns with 30% rubberized concrete. The columns were tested under pendulum impact until failure.

Mix design and pre-treatment

Three concrete mixes were designed to examine the effects of varying rubber contents on the impact resistance of reinforced concrete columns. The conventional concrete served as a baseline had the compressive strength of 50 MPa. Normal fine and coarse aggregates of the rubberized concrete were replaced by rubber at 15% and 30%, in which conventional aggregates were replaced by two types of rubber aggregates including 2-5 mm diameter crumbed rubber and 5-7 mm diameter crumb rubbers. The crumbed rubber was manufactured and supplied by tyre cycle [24]. The crumb rubber has the specific gravity of 540 kg/m^3 [1]. The sieve tests were carried out and the particle size distribution is shown in Fig. 1. All the specimens had the ratios of cement, water and total aggregate remain unchanged. The ratio of water to cement was 0.5 for all the mixes. It is noted that the rate at which water was added to the mix had a large impact on the slump and mixing of the concrete. Gradually adding water to the mixer produced the

best result as it reduced clumping of material and ensured a good distribution of water. The water absorbed by rubber through the water soaking process was accounted for when producing rubberized concrete by deducting the overall water required for the mix by the amount of absorbed water. Details of the mixture design of the rubberized concrete are presented in Table 1. The compressive strength of rubberized concrete was tested at 28 days according to AS 1012.9 [25]. The compressive strengths of 0%, 15%, and 30% rubberized concrete were 50.3 MPa, 25.0 MPa, and 14.4 MPa, respectively. The density of the specimens was 2271 kg/m^3, 2086 kg/m^3, and 1943 kg/m^3, respectively.

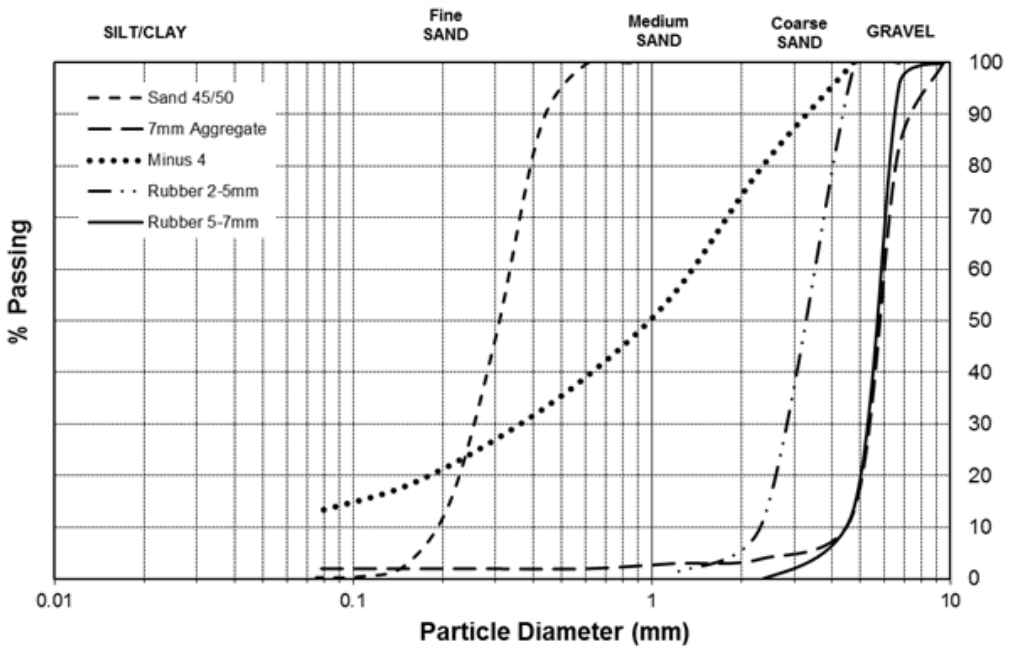

Fig. 1. Particle size distribution from sieve testing

According to a previous study by Mohammadi [26], rubber aggregates for the two mixes were soaked for 24 hours in a 10% sodium hydroxide solution (NaOH). This process allows the aggregates to absorb a certain amount of water, improving the interfacial bonding and reducing the possibility of rubber aggregate floating in the mix. After the treatment, the rubber was drained, then soaked and rinsed three times in clean water to neutralize the pH. As mixing the concrete, the rubber aggregates and the conventional aggregates were mixed for 1 minute with 10% of the required water, then cement was added and the substances are mixed for 1 minute.

Next, a half of the remaining water was added and mixed for 1 minute. Lastly, the remaining amount of the water was added and mixed for 1 minute before adding superplasticizer and mixing for 1 minute. Details about the mixing procedure can be found in the previous study by Elchalakani [1]. Slump tests were carried out for each mix and the slump of normal concrete, 15% rubberized concrete and 30% rubberized concrete was 150 mm, 180 mm, and 165 mm, respectively.

Specimen design

Figure 2 shows the schematic view of the specimen and the experimental pendulum impact test setup. The overall dimensions of the testing column were 800 mm in height and 100 mm x 100 mm in cross-section area. A footing of 140 mm depth and 400 mm x 400 mm in cross-section area was built to connect the column specimens to the laboratory strong floor. The solid steel impactor weight was 300 kg. The added mass on top of the column specimen was made of 288 kg and consisting of 400 mm x 400 mm x 450 mm (L x W x H) concrete block and 5 pieces of 23 kg steel plates that were firmly fixed to the top slab. The total weight of added mass is thus 403 kg. It should be noted that road side barriers normally do not support vertical load. Adding a dead weight generates initial compressive stress and also the P-Δ effect on the column, which may lead to conservative test results if the damage is governed by tensile strength of the column owing to flexural bending. In this study, however, the dead weight was added in the tests to simulate the vertical downward load as recommended in the standard AS 5100.2:2017 [27] in which road side barriers are classified based on its performance level, such as low, regular, and medium performance levels. For the regular barrier performance level, the ultimate vertical downward load of 100 kN over 6 m contact length between the barrier and the vehicle as given in Table 12.2.2 of AS 5100.2:2017 [27]. The compressive strength of concrete material with 0% rubber at the testing day was 50.3 MPa.

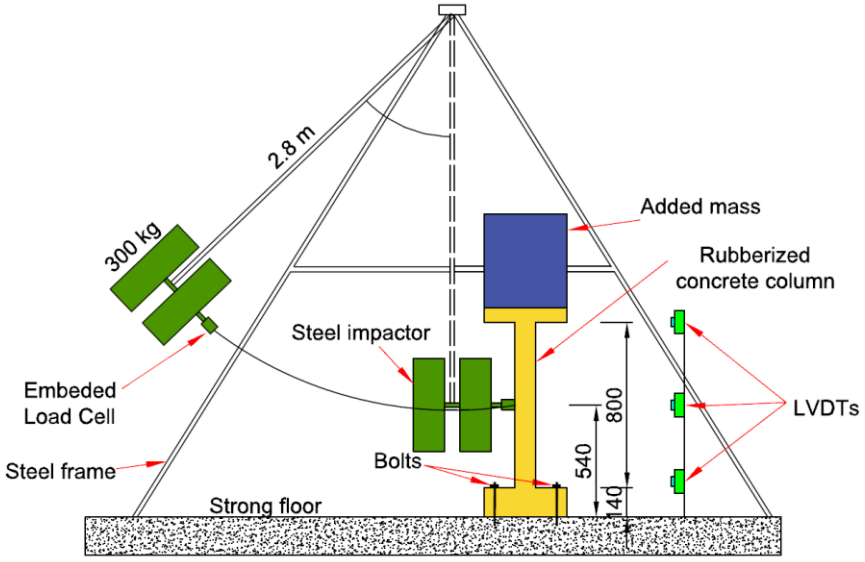

Fig. 2. Impact test setup

The reinforcement of the columns included 6 mm diameter bars in the longitudinal direction and 4 mm diameter stirrups at a spacing of 50 mm throughout the columns. The longitudinal reinforcement ratio of these columns was 1.14%. The 6 mm diameter longitudinal bars were extended into the top flange and the bottom footing to create fully fixed boundary conditions at the two ends. The nominal yield stress and elastic modulus of the reinforcement were 250 MPa and 200 GPa, respectively.

In addition, there was one 15% rubberized concrete column confined with CFRP. Column CF-15-01 was wrapped with one longitudinal CFRP layer and one transverse CFRP layer. It should also be noted that the transverse layers had an overlap of 100 mm. Carbon fiber SikaWrap®-230C which is a woven unidirectional carbon fiber fabric designed for structural engineering applications was used in this study. The dry fiber had the tensile strength of 4300 MPa as provided by the manufacturer [28]. The fiber density was 1.8 g/cm^3 and the nominal thickness was 0.131 mm. The dry fiber modulus of elasticity in tension was 230 GPa. Firstly, the concrete surface of the two columns was prepared carefully in which all grease, dust, and any other contaminant that could impair adhesion were removed by an air jet. The concrete surface was

177 then cleaned by acetone before bonding with FRP. The epoxy curing time was maintained at
178 least seven days before testing. Epoxy MasterBrace 4500 was used to bond FRP to concrete
179 surface. The epoxy consisted of two parts with the mixing ratio of 2:1 by weight as
180 recommended by the manufacturer [29]. The epoxy had the nominal tensile strength = 17 MPa,
181 compressive strength = 60 MPa, and flexural strength = 35 MPa. The first coat of epoxy should
182 be applied to the concrete surface using either a roller or brush. The CFRP sheet was placed on
183 the concrete surface and rolled in the fiber direction two to three times using a Uni-Pro fiber
184 glass compression roller [30] to impregnate the resin into the fibers. This process was done to
185 ensure no air bubbles in the interfaces and the resin. It should be noted that when joining strips
186 of fiber together a 15 cm overlap length is required in the main direction and additional resin
187 must be applied at the overlap section.

188 ***Impact test setup***

189 The pendulum impact apparatus comprised a steel rig fixed on a strong solid floor to support
190 the entire test system. A 300-kg solid steel impactor was connected through a 2.8-m-long steel
191 arm to the frame. An inclinometer installed on top of the steel rig was utilized to measure the
192 release angle of the impactor. For each impact test, the impactor was lifted to a certain height,
193 corresponding to a designated angle, and then released to impact the centre (mid-height) of the
194 columns. The impactor hits the column and rebounds, which is pulled back to avoid the column
195 being impacted for the second time.

196 The impact force was measured by a load cell that was fixed in front of the impactor. One linear
197 variable differential transformer (LVDT) was placed at column mid-height to confirm the
198 displacements recorded by the high-speed camera. The load cell and LVDT were connected to
199 a National Instrument USB-9237 acquisition system, and the data were captured at a sampling
200 frequency of 50 kHz. A high-speed camera (Photron SA-Z) was utilized to monitor the

deformation-to-failure process of the columns. The filming rate of the high-speed camera was set to 8000 frames per second and the exposure time was set to balance with the aperture. Four halogen lights were used to provide sufficient lighting for high-speed filming. Seven tracking points were used for the columns to enable the high-speed camera images to be post-processed using digital image correlation software to derive the column displacement time histories at these tracking points. The tracking points are spread apart at 100 mm with an extra point on the impactor and on the top of the column.

Experimental results and discussion

The columns were tested with multiple impacts by progressively increasing the impact velocity. The release angle of the steel projectile was 3^o, 15^o, and 30^o which corresponded to Impact 1, 2, and 3 with the impact velocities of 0.27 m/s, 1.37 m/s, and 2.71 m/s, respectively. In addition, if the columns did not fail at the third impact, they were subjected to the fourth impact which was released at an angle of 40^o, corresponding to the impact velocity of 3.58 m/s. The progressive failure of the columns was examined by using the high-speed camera. Accordingly, the images from the high-speed camera were used to conduct image processing for measuring the displacement and velocity at multiple points. Meanwhile, the impact force was monitored by using the mounted load cell on the steel impactor.

Deformation and progressive failure

In general, all the columns exhibited hairline cracking at the midpoint (impact point) and near the top and bottom footings after Impact 1. These cracks had clearly developed and propagated after Impact 2. Subsequently, these columns experienced severe damage associated with varying degrees in which major cracks or complete collapse of the columns were observed. All of the columns failed after the third impact. The impact response of the columns included two

stages: the first stage is the impact force phase when the impactor and the column were in contact and the second stage when the columns freely vibrated after the impactor and the columns were apart. The first stage lasted for about 40-80 ms which is the impact duration in the impact force time history while the free vibration phase lasted much longer up to 1 second.

The deformation and the progressive failure of the specimens were recorded by the high-speed camera and presented in Fig. 3. This figure shows the response of Columns CT-15-02 and CF-15-01 after Impact 3. For Column CT-15-02, the flexural crack at the rear face of the column caused failure followed by cracks at the columns top and base. It is different from the static case, when the columns were impacted, the added mass on the top provided inertial restraint to the column and acted as a fix restraint at the column top in the early stage of the impact event. This observation was also reported in the previous studies [31, 32]. On the other hand, Column CF-15-01 failed by noticeable damage of the two ends of the column where the joint between the column and the top and base concrete blocks opened with longitudinal reinforcements fractured. The damage at the two ends of Column CF-15-01 was more severe than that of Column CT-15-02. FRP confinement enhanced the column strength at the impact point so that it did not fail under Impact 3. The mid-height region of Column CF-15-01 observed less impact energy than that of Column CT-15-01. As a result, more impact energy was transferred to the two ends of Column CF-15-01 and thus caused more serious damage. It is noted that the vibration and displacement of the columns under Impact 1 and 2 are not presented here since the small impact forces did not cause any remarkable damage. However, the image processing was carried out by using high-speed camera images to investigate the lateral displacement at the tracking points.

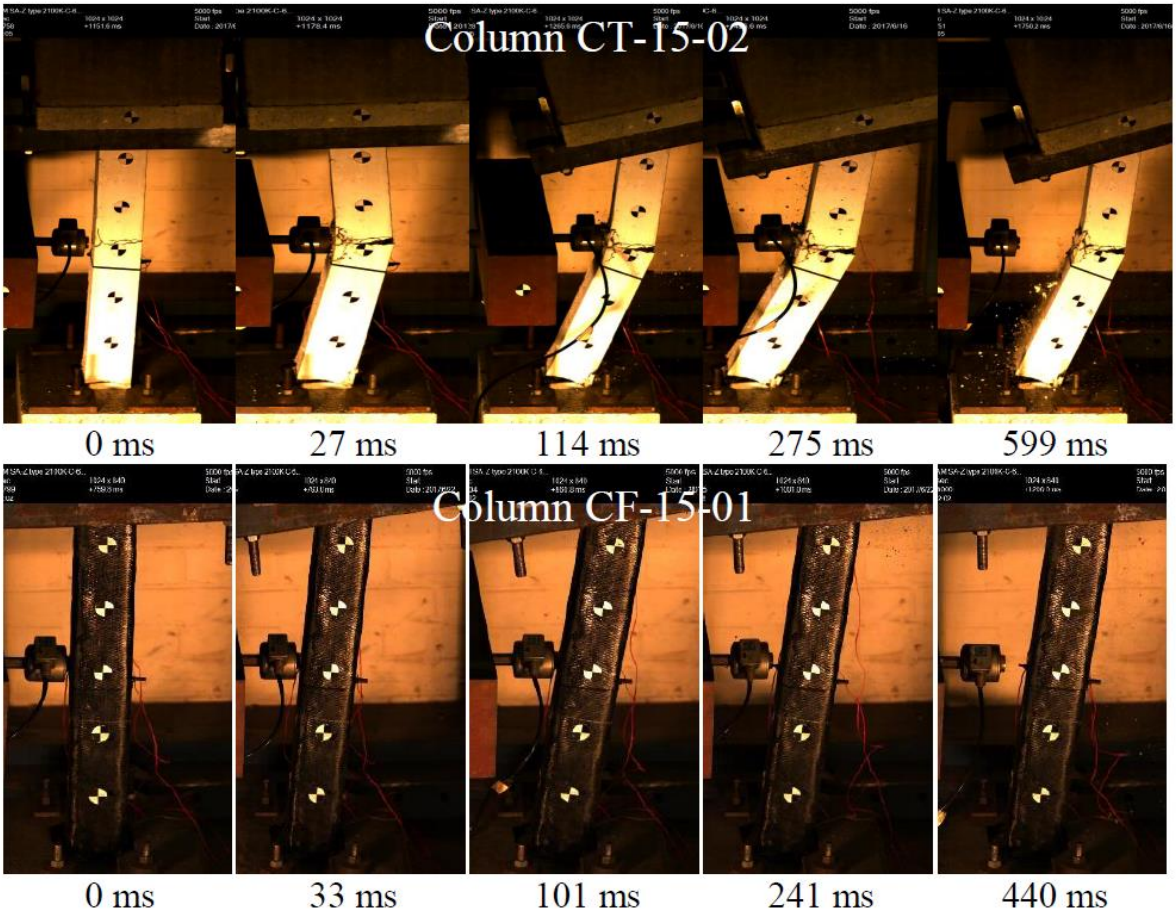

Fig. 3. Impact response of Column CT-15-02 (above) CF-15-01 (below) under Impact 3

The typical failure of the unconfined rubberized concrete columns is described in Fig. 4 where damage was observed at three critical sections including the impact point, the column-footing connection, and the column-top connection. The failure of these columns was caused by both flexural and shear failure. Damage to the columns was found to be localized at the three critical locations while there was no damage at other parts of the columns. As the impact force was increased, concrete crushing at the impact point and flexural damage of concrete in the rear face of the columns were observed. Diagonal shear damage near the column base and column top was also initiated after Impact 2. As shown in Fig. 3, the flexural crack at the impact point was very severe at 27 ms while the top concrete plate was still perpendicular to the column indicating that only minor cracks appeared and no damage was observed. Accordingly, damage of the three critical locations became obvious at 114 ms. As the impact force increased, the

shear and flexural cracks further increased leading to complete failure of the columns. At the same level of the impact, the columns with higher rubber content showed more severe damage.

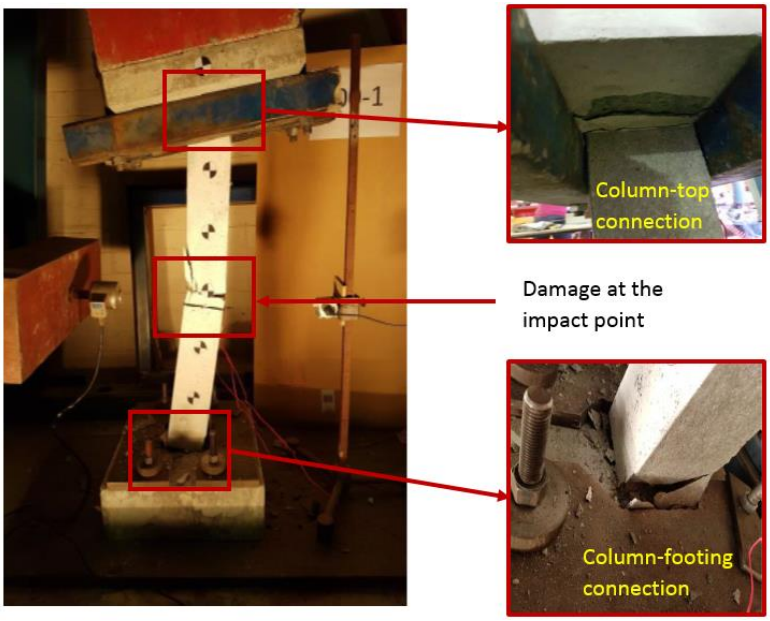

Fig. 4. Typical failure of the columns under lateral impact (CT-30-01)

The damage and failure mode of the tested columns with different rubber contents are shown in Fig. 5 to investigate its effect on the failure mode. As can be seen from the figure, the level of damage increases with the rubber content. It mean that the columns with higher rubber content exhibited more severe damage and thus absorb more impact energy. The use of FRP confinement has changed the failure mode of the rubberized concrete columns from three-plastic-hinge to two-plastic-hinge failure. However, the confined column was stronger than other columns so that it survived after impact 3 and failed at Impact 4 under higher impact energy.

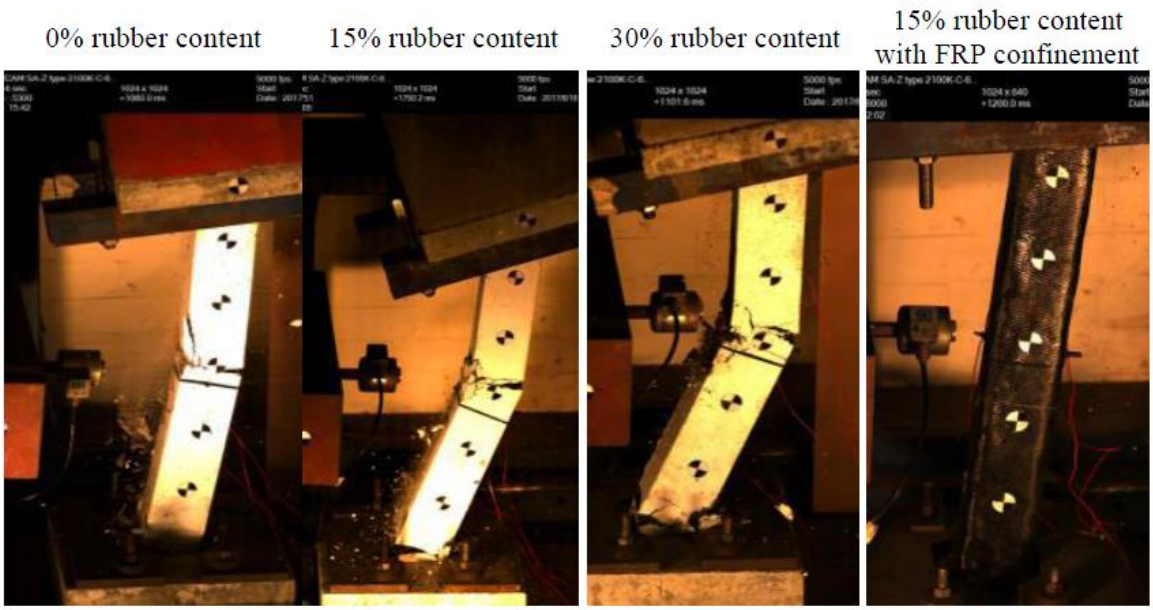

Fig. 5. Damage of the tested columns with different rubber contents after Impact 3

Impact force time histories

Impact force time histories of the rubberized concrete columns were derived from the load cell record and shown in Figs. 6-7. All the graphs exhibit a similar pattern including an initial peak followed by a subsequent peak caused by the interaction between the impactor and the column. The first peak impact force was significantly larger than other peaks and the impact duration during the first peak was about 30 ms for the normal concrete columns and 40-60 ms for the rubberized concrete columns. As displayed in the graphs, with the increase in the release angle from 3 degree to 15 degree, the peak impact force showed a significant increase. However, the peak impact force of the unconfined rubberized concrete columns did not further increase when the release angle increased from 15 degree to 30 degree. On the other hand, the peak impact force of all the rubberized columns under Impact 3 was smaller than Impact 2 except the confined column CF-15-1. It was because Impact 2 caused damage at the impact point to the column and reduced the contact stiffness of the columns so that the impact force was smaller although the impact kinetic energy is larger. It is noted that the impact force time history of

Column CF-15-01 under impact 2 was missed due to a malfunction but the peak was seen at about 32 kN. The rubberized concrete confined with FRP exhibited a significant increase in its impact load resistant capacity as shown in Fig. 7.

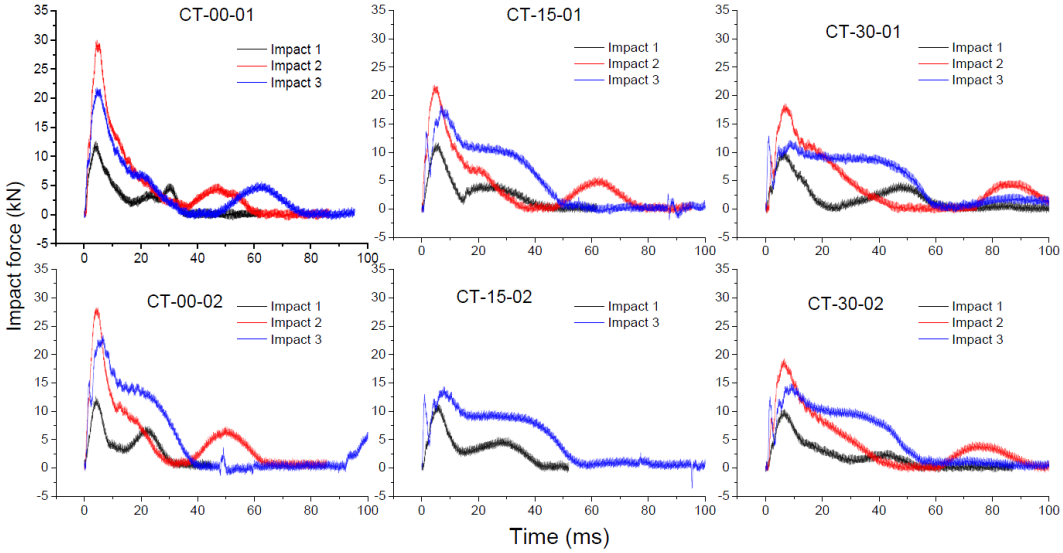

Fig. 6. Impact force time histories of the columns

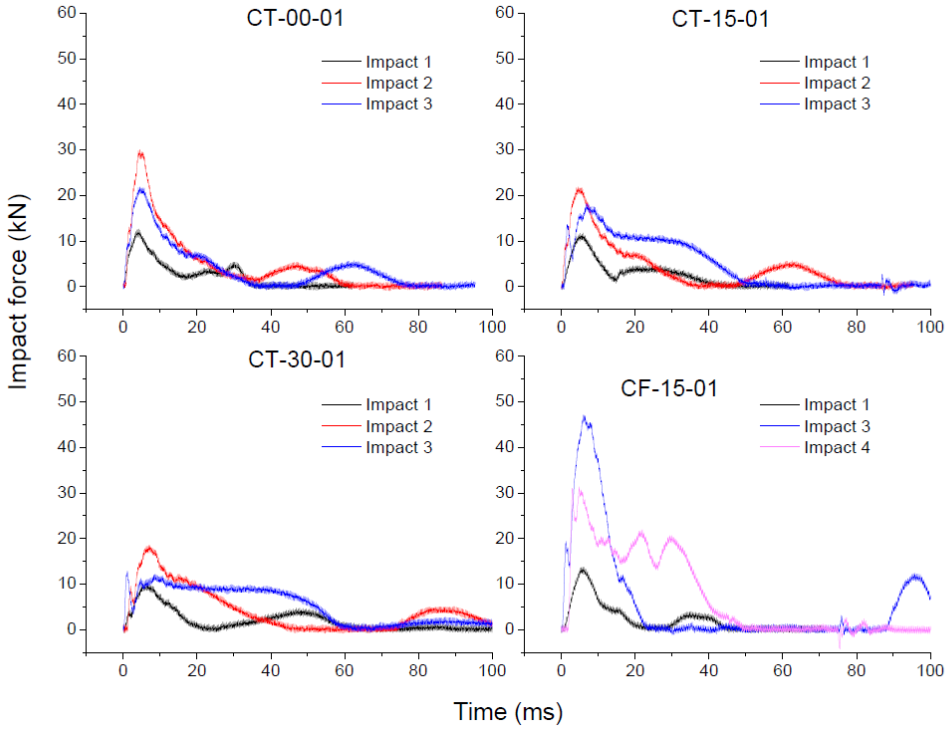

Fig. 7. Impact force time histories of the columns with and without FRP confinement

As shown in Fig. 6, the impact force time histories among the three impacts exhibited a slight difference at the second peak. For Impact 2, there was a gap between the first and the second impact with the impact force equal to zero, implying the impactor and the column separated from each other before the column rebounded back inducing the second impact. Meanwhile, this phenomenon was not observed for Impact 1. As the impact energy was relatively small (Impact 1), after the first contact the impact force reduced owing to the deformation of the column but the impactor moved together with the column before column rebounded to induce the second impact. As the impact energy and impact forces increased, the impactor pushed the column to deform quickly and at the same time the larger impact caused more prominent rebound of the impactor, which resulted in separation between the impactor and the column before column rebounded to cause the second impact. Close inspections on the high-speed camera images have confirmed that the columns rebounded and made contact with the load cell causing the second peak. The peak impact force and impact duration of the columns are presented in Table 2. In addition, the impact impulse is estimated as the enclosed area of the impact force time history and also presented in the table.

Fig. 6 shows the rubberized concrete significantly reduced the peak impact force and extended the impact duration. For instance for Impact 2, the peak impact forces of Columns CT-00-01, CT-15-01, and CT-30-01 were 30 kN, 22 kN, and 18 kN, respectively, corresponding to the reduction of the peak impact force by 27% and 40%. In the meantime, the duration of these impacts was 60 ms, 80 ms, and 110 ms for Columns CT-00-01, CT-15-01, and CT-30-01, respectively. It is noted that the impact duration of these columns includes the first and the second peak impact force as shown in Fig. 8. The impact force time histories after Impact 2 showed the highest impact forces so that it was chosen to compare the impact resistance between the columns with different rubber contents. This characteristic has proven that rubberized concrete can be efficiently utilized in real structures to minimise the peak impact

force. For example, rubberized concrete can be used as road side barriers to considerably reduce peak impact force and thus minimize injury or even death when an accidental collision occurs. However, as shown in Fig. 8, the impact load resistant capacity of the rubberized concrete columns is smaller than that of the reference column. A compromise between the energy absorption and the load resistant capacity is required when designing these structures.

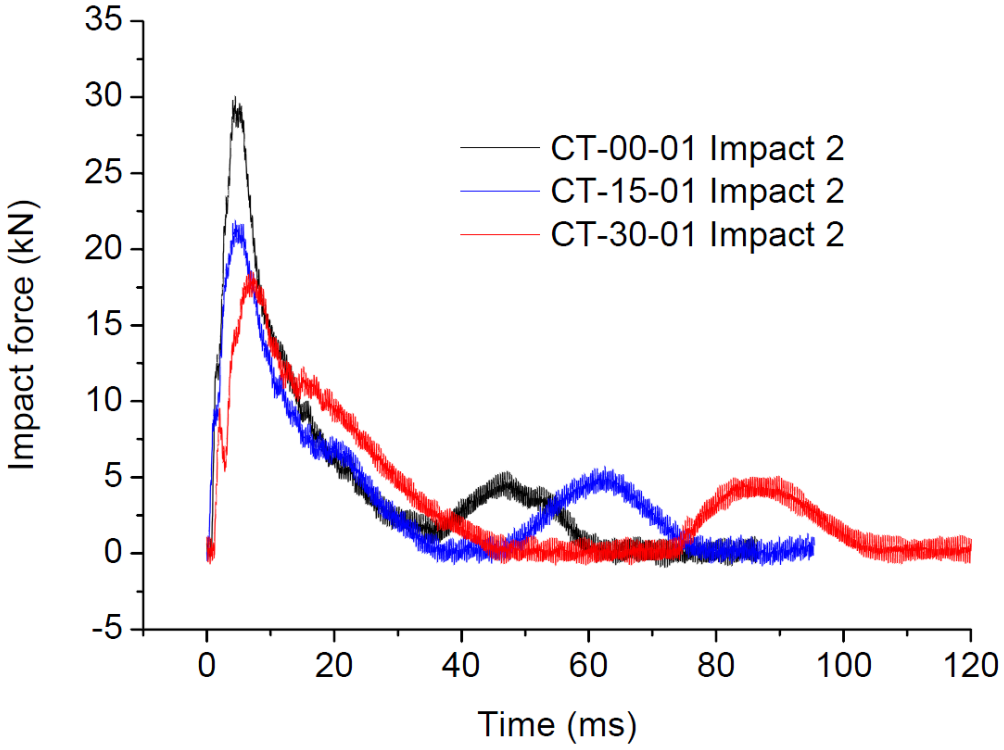

Fig. 8. Impact force time histories of the columns with different rubber contents under impact 2

Displacement time histories

The displacement time histories of the columns were derived from image processing of the high-speed camera images at the tracking points including the midheight and column top as shown in Figs. 9-10. In addition, the maximum displacement at the midheight and the column top as well as the residual displacement are presented in Table 3.

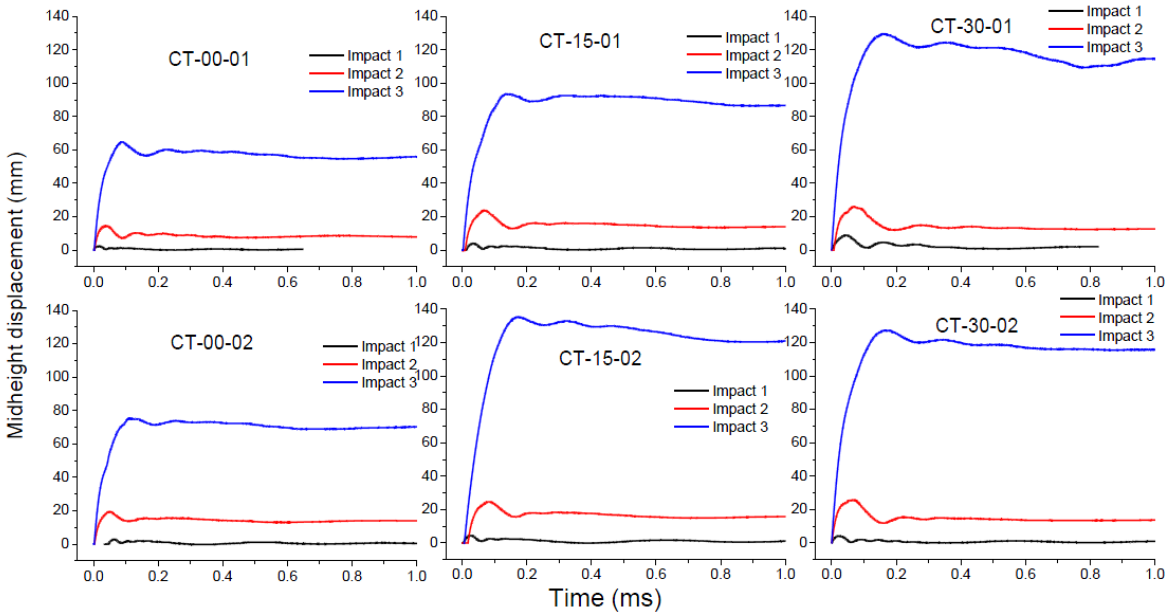

Fig. 9. Midheight displacement histories of the columns

As shown in Fig. 9 and Table 3, the maximum displacement of the columns under Impact 1 was quite small and the columns' deformation was mostly still in the elastic range and the residual displacement of these columns ranged from 0.5 mm to 1.5 mm. As the impact energy increased (Impact 2), the maximum displacement at the impact point of normal concrete columns was 15-19 mm while the corresponding values of the columns with 15% and 30% rubber contents were 23-25 mm, and 25-26 mm, respectively. These results demonstrate that rubberized concrete columns become much flexible than its counterpart made of normal concrete. As can be seen from Fig. 9 and Table 3, the column displacement increased significantly when the rubber contents increased from 0% to 15%. However, further increasing the rubber content from 15% to 30% did not change the column displacement considerably. Under Impact 3, the maximum displacement of Column CT-00 at the impact point was 65-75 mm while the corresponding values for Column CT-15 and CT30 were 92-137 mm and 127-130 mm, respectively. The rubberized concrete columns deflected approximately twice the reference columns CT-00 (≈70 mm vs ≈120 mm).

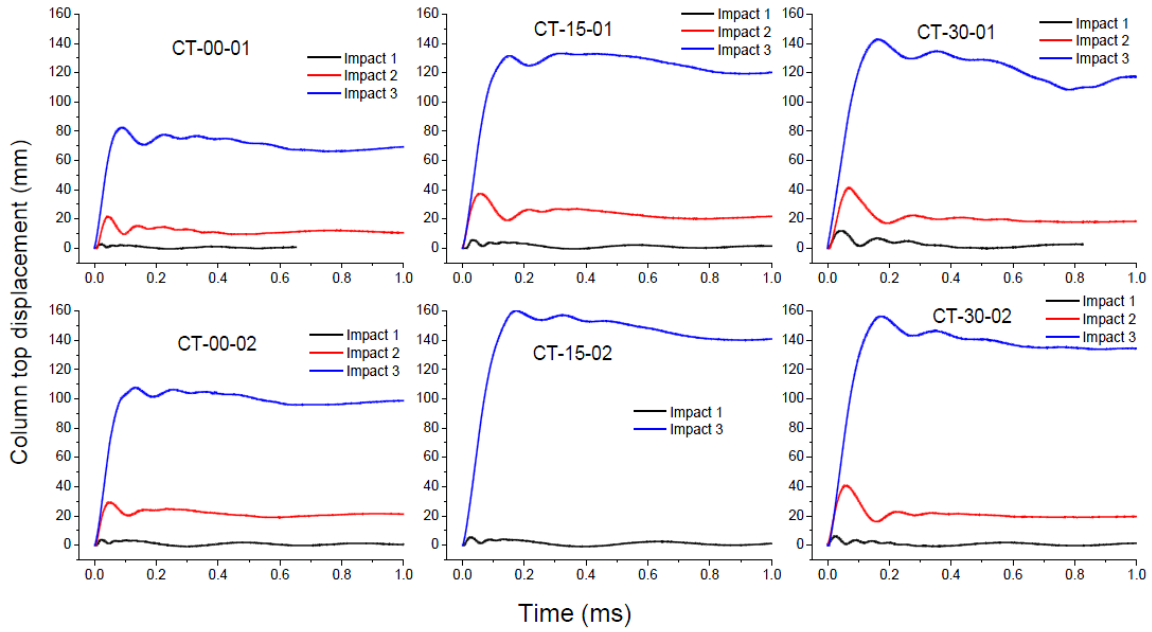

Fig. 10. Column top displacement time histories

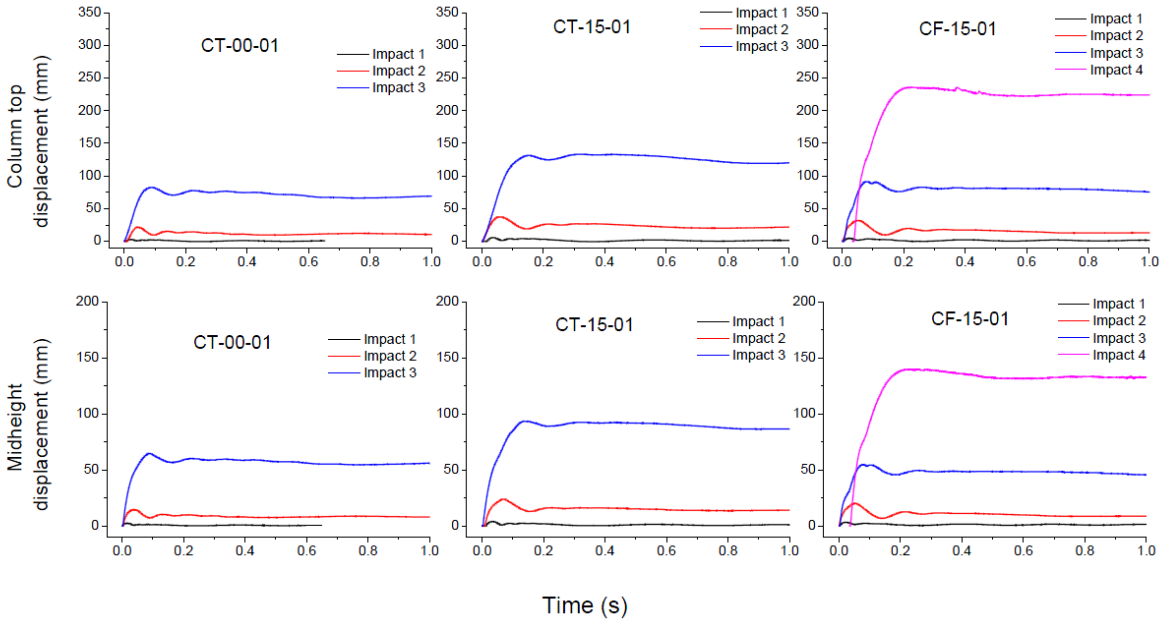

Fig. 11. Displacement time histories of the columns with and without FRP confinement

Fig. 11 shows the effectiveness of using FRP confinement to reduce the displacement. Under Impact 2, the maximum displacement at mid-height of the normal concrete columns was 15-19 mm while the corresponding displacements for two Columns CT-15 and Column CF-15-01 were 23-25 mm and 20 mm, respectively. Column CF-15-01 did not show a considerable

356 enhancement of the column's stiffness under Impact 2 compared to the reference column. The
357 rubber content in Column CF-15-01 made the column more flexible while the FRP confinement
358 increased the column stiffness and partially compensated for the loss of the column's stiffness
359 due to replacing aggregates with rubber. As a result, the column CF-15-01's displacement was
360 in between the reference plain concrete column and column CT-15. Under Impact 3, the
361 midheight displacement of the reference columns (CT-00) was 65-75 mm while the
362 corresponding midheight displacement of Columns CT-15 and CF-15-1 were 92-137 mm and
363 55 mm, respectively. It can be seen that the FRP confinement can significantly reduce the
364 displacement while it still enhance the energy absorption capacity. As shown in Table 2, the
365 energy absorption of Column CT-00-01 and CF-15-01 under Impact 3 was 517 J and 821 J,
366 respectively.

367 In addition, the displacement time histories at the column top (Fig. 10) is also an important
368 measure of the column response under lateral impact. It is different from the static case, where
369 the displacement at the column top is 2.5 times the displacement at the midheight, the
370 displacement at the column top was almost similar to that at the impact point but with a delay.
371 This delay relates to the free vibration frequency of the columns and also the interaction
372 between the impactor and the columns, which generated stress waves travelling from the impact
373 point toward the column ends. From Fig. 12, the vibration period of Column CT-00 was
374 approximately 270 ms, which is estimated from the free-vibration phase of the testing results
375 from Impact 1. The natural vibration period of these columns can be theoretically estimated as
376 235 ms. These results have confirmed the reliability of these complicated impact tests. The
377 natural vibration period can be estimated as follows [31, 32]:

378
$$T = 2\pi \sqrt{\frac{m + m_{add}}{\frac{3EI}{(L + H_T)^3}}} = 235\ (ms) \qquad (1)$$

where m and m_{add} are the total mass of the column and the added mass, respectively, k is the stiffness of column under lateral static load, E is Young's modulus of concrete material, $4700\sqrt{f_c}$, f_c is the compressive strength of concrete, i.e. 50 MPa in the present study; I is the moment of inertia, L is the length of the column, and H_T is the height of the lumped block.

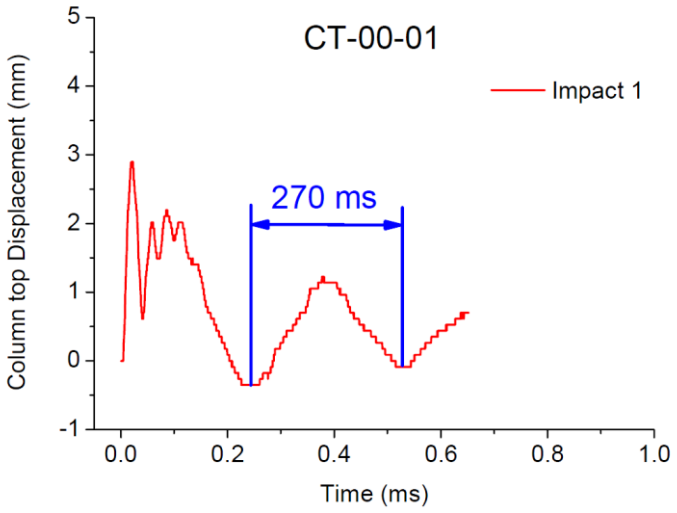

Fig. 12. Natural vibration period of Column CT-00-01

It is noted that Column CT-00-01 under Impact 1 was chosen to verify the vibration period because the column's deformation was still in the elastic range associated with small displacement and deformation. In addition, the elastic modulus of the normal concrete can be easily and accurately estimated from available formula in the literature while there is no equation to accurately estimate the elastic modulus of the rubberized concrete.

Energy absorption

The energy absorption is an important factor when examining the impact resistance capacity of the columns. The energy absorption is dependent on the impact force and the displacement of the columns. Fig. 13 shows the impact force versus the midheight displacement of the columns for each impact. The enclosed area by the force-displacement curve indicates the energy absorption through the column deformation and damage as summarized in Table 2. As shown in Fig. 13, the impact force of the normal concrete columns was higher than those of the

rubberized concrete columns. However, the deformations of the latter ones were significantly larger. When the impact force was small and the columns deformation was mostly in the elastic range, the energy absorption of the rubberised concrete columns was higher than that of the reference columns. For Impact 1, the impact energy absorption of Columns CT-15 and CT-30 are 42% and 130% higher the reference columns, respectively. For Impact 2, the corresponding values for Columns CT-15 and CT-30 were 4% and 6%. For impact 3, the energy absorption of the columns without rubber was approximately 607 J while the corresponding average energy absorption for the columns with 15% and 30% rubber was 683 J and 867 J, respectively. These increases indicate that the enhancement of energy absorption in these columns was 13% and 43%, respectively. Therefore, it can be concluded that rubberized concrete increases the energy absorption under lateral impact forces.

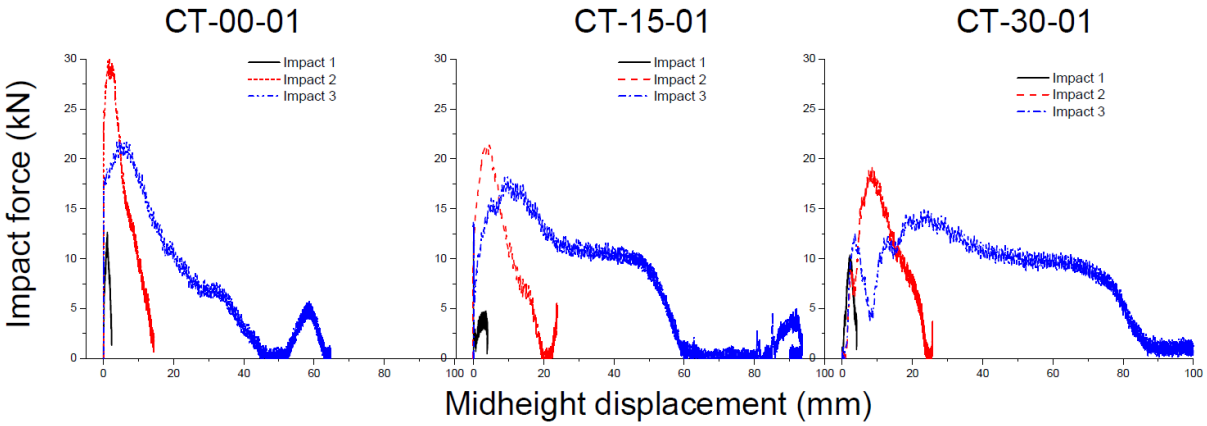

Fig. 13. Impact force versus mid-height displacement of the rubberized concrete columns

Fig. 14 shows the impact force versus the midheight displacement of the columns for each impact. The rubberized concrete column confined with FRP exhibited an exceptional improvement in absorbing energy. Under the first impact, the energy absorption of Columns CF-15-01 was enhanced by 107% as compared to that of the reference column. As mentioned previously, this column survived after the third impact with the release angle of 30^{o} and it is the only column failing at the fourth impact with the release angle of 40^{0}. The maximum energy absorption of Column CF-15-01 at the fourth impact was 1483 J which was equal to 2.44 times

the corresponding one of the reference column (607 J). Therefore, FRP confined concrete column can be used to achieve both better energy absorption and load carrying capacity.

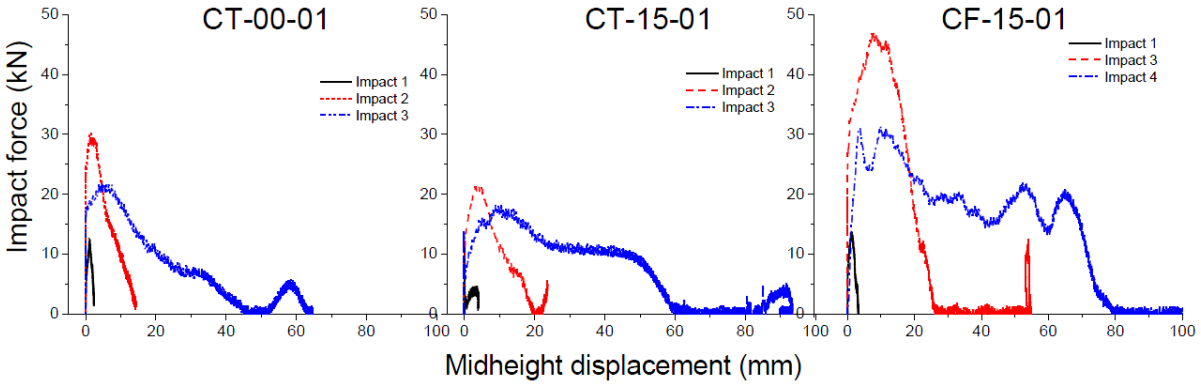

Fig. 14. Impact force versus mid-height displacement of the columns with/without FRP confinement

Conclusions

The impact behaviour of rubberized concrete columns has been experimentally investigated by using the pendulum impact tests. The rubberized concrete columns showed an excellent impact behaviour over the normal concrete columns. The key findings can be summarized as follows:

1. The rubberized concrete columns significantly reduce the peak impact force (27% - 40%) and thus they can mitigate the risk of injury if rubberized concrete is used in construction of roadside barriers.

2. The rubberized concrete columns are more ductile and they can deflect twice the reference columns before failure, especially when they are confined with FRP.

3. Rubberized concrete significantly increases the impact energy absorption. The columns with 15% and 30% rubber showed an increase in the impact energy absorption by 58% and 63% as compared to the reference columns, respectively.

4. The rubberized concrete columns with and without FRP confinement showed an increase of the impact energy by 4-42% and 35-144% as compared to the reference columns, respectively.

Finally, the results in this study has indicated that rubberized concrete is a promising material to use in roadside barriers since it significantly increases the ductility and energy absorption under impact loads. In addition, rubberized concrete considerably reduces the peak impact force and thus it can reduce the risks to passengers if collision occurs.

Acknowledgement

The authors would like to deeply thank Liam O'keefe from Tyres Stewardship Australia and Adrian Jones from Tyrecycle. Thanks are given to Andrew Sarkady and Anup Chakrabortty from BASF for kindly donating the superplasticizer required for all the specimens. Thanks are given to the following technicians Matt Arpin, Malcolm Stafford, Jim Waters and Brad Rose for assisting the students in performing the experiments. Thanks are given to Cameron Marshal and Armin Hosseini, and David Pegrum, former students of the University of Western Australia for performing the tests and processing the test data.

References

[1] Elchalakani M. High strength rubberized concrete containing silica fume for the construction of sustainable road side barriers. Structures. 2015;1:20-38.
[2] Topçu IB. The properties of rubberized concretes. Cem Concr Res. 1995;25(2):304-10.
[3] Topçu IB, Avcular N. Collision behaviours of rubberized concrete. Cem Concr Res. 1997;27(12):1893-8.
[4] Khatib ZK, Bayomy FM. Rubberized Portland cement concrete. J Mater Civ Eng. 1999;11(3):206-13.
[5] Hernández-Olivares F, Barluenga G, Bollati M, Witoszek B. Static and dynamic behaviour of recycled tyre rubber-filled concrete. Cem Concr Res. 2002;32(10):1587-96.
[6] Atahan AO, Sevim UK. Testing and comparison of concrete barriers containing shredded waste tire chips. Mater Lett. 2008;62(21):3754-7.

[7] Ozbay E, Lachemi M, Sevim UK. Compressive strength, abrasion resistance and energy absorption capacity of rubberized concretes with and without slag. Mater Struct. 2011;44(7):1297-307.
[8] Liu F, Chen G, Li L, Guo Y. Study of impact performance of rubber reinforced concrete. Constr Build Mater. 2012;36:604-16.
[9] Gupta T, Chaudhary S, Sharma RK. Assessment of mechanical and durability properties of concrete containing waste rubber tire as fine aggregate. Constr Build Mater. 2014;73:562-74.
[10] Youssf O, Hassanli R, Mills JE. Mechanical performance of FRP-confined and unconfined crumb rubber concrete containing high rubber content. Journal of Building Engineering. 2017.
[11] Pham TM, Elchalakani M, Hao H. Axial impact resistance of rubberized concrete with/without FRP confinement for sustainable road side barriers. Int J Protect Struct. 2018;Revision submitted.
[12] Zheng L, Sharon Huo X, Yuan Y. Experimental investigation on dynamic properties of rubberized concrete. Constr Build Mater. 2008;22(5):939-47.
[13] Sukontasukkul P, Chaikaew C. Properties of concrete pedestrian block mixed with crumb rubber. Constr Build Mater. 2006;20(7):450-7.
[14] ACI 544.2R-17. Report on the Measurement of Fresh State Properties and Fiber Dispersion of Fiber-Reinforced Concrete. Farmington Hills, MI: American Concrete Institute; 2017.
[15] Atahan AO, Yücel AÖ. Crumb rubber in concrete: Static and dynamic evaluation. Constr Build Mater. 2012;36:617-22.
[16] Donga PD, Shah D, Bhavsar JK. Impact Resistance of Waste Rubber Fiber Silica Fume Concrete. Journal of Civil Engineering and Environmental Technology. 2016;3(4):274-9.
[17] Gupta T, Sharma RK, Chaudhary S. Impact resistance of concrete containing waste rubber fiber and silica fume. Int J Impact Eng. 2015;83:76-87.
[18] Youssf O, ElGawady MA, Mills JE. Static cyclic behaviour of FRP-confined crumb rubber concrete columns. Eng Struct. 2016;113:371-87.
[19] Xue J, Shinozuka M. Rubberized concrete: A green structural material with enhanced energy-dissipation capability. Constr Build Mater. 2013;42:196-204.
[20] Sukontasukkul P, Jamnam S, Rodsin K, Banthia N. Use of rubberized concrete as a cushion layer in bulletproof fiber reinforced concrete panels. Constr Build Mater. 2013;41:801-11.
[21] Pham TM, Chen W, Hao H. Failure and impact resistance analysis of plain and FRP-confined concrete cylinders under axial impact loads. Int J Protect Struct. 2018;9(1):4-23.
[22] Pham TM, Hao H. Axial impact resistance of FRP-confined concrete. J Compos Constr. 2017;21(2):04016088.
[23] Pham TM, Hao H. Behavior of fiber reinforced polymer strengthened reinforced concrete beams under static and impact loads. Int J Protect Struct. 2017;8(1):1-22.
[24] Tyre recycle. 2018.
[25] AS 1012.9. Compressive strength tests - concrete. 10129: 2014. Sydney, NSW, Australia2014.
[26] Mohammadi I. Investigation on the use of crumb rubber concrete (CRC) for rigid pavements 2014.
[27] AS 5100.2:2017. Bridge design. Part 2: Design loads. Sydney, NSW, Australia2017.
[28] Sika Australia. Strengthening columns or beams with carbon fibre fabric. 2017.
[29] BASF. MasterBrace 4500 - High strength saturant for MasterBrace fabric sheets. 2017.
[30] Uni-Pro. UNi-PRO Fibreglass Compression Roller. 2017.
[31] Do TV, Pham TM, Hao H. Numerical investigation of the behaviour of precast segmental concrete columns subjected to vehicle collision. Eng Struct. 2018;156:375-93.
[32] Do TV, Pham TM, Hao H. Dynamic responses and failure modes of bridge columns under vehicle collision. Eng Struct. 2018;156:243-59.

511 **List of Figures**

List of Tables

531 Table 1. Mix design and preliminary test results

% rubber	Water (kg/m^3)	Cement (kg/m^3)	4-7 mm agg. (kg/m^3)	<4 mm agg. (kg/m^3)	Sand (kg/m^3)	Rubber 5-7 mm (kg/m^3)	Rubber 1-5 mm (kg/m^3)	f_c' (MPa)
0	213	426	750	130	843	0	0	50.27
15	213	426	638	111	717	49	63	23.67
30	213	426	525	91	590	98	127	14.37

532

533 Table 2. Impact force and energy dissipation of the tested columns

Column	Impact	Peak impact force (kN)	Impact duration (ms)	Impulse (kN.ms)	Energy dissipation (J)
CT-00-01	1	13	40	161	19
	2	30	60	416	228
	3	21	110	701	517
CT-00-02	1	13	40	167	9
	2	28	80	439	233
	3	23	125	627	697
CT-15-01	1	12	50	171	12
	2	22	80	381	140
	3	17	150	593	691
CT-15-02	1	11	50	180	27
	2	N.A	N.A	N.A	N.A
	3	14	150	591	676
CT-30-01	1	10	80	211	39
	2	18	110	444	235
	3	13	250	644	849
CT-30-02	1	10	80	176	25
	2	19	100	433	253
	3	15	250	693	885
CF-15-01	1	14	50	1645	29
	2	N.A	N.A	N.A	N.A
	3	46	25	634	821
	4	32	50	824	1483

534

535 Table 3. Peak and residual displacement of the columns

Column	Impact	Peak Disp. at column top (mm)	Residual Disp. at column top (mm)	Peak Disp. at midheight (mm)	Residual Disp. at midheight (mm)
CT-00-01	1	2.7	0.5	2.7	0.5
	2	22.0	10.0	14.5	8.5
	3	82.0	72.0	65.0	58.0
CT-00-02	1	3.8	0.6	2.9	0.4
	2	29.0	20.0	19.0	14.0
	3	108.0	97.0	75.0	70.0
CT-15-01	1	5.6	1.0	4.0	0.6
	2	37.5	22.5	23.0	14.0
	3	130.0	125.0	92.0	87.0
CT-15-02	1	5.5	1.0	4.5	0.9
	2	N.A	N.A	24.8	15.2
	3	160.0	142.0	137.0	122.0
CT-30-01	1	12.0	1.3	9.0	1.5
	2	41.0	19.0	26.0	13.0
	3	142.0	118.0	130.0	118.0
CT-30-02	1	6.0	0.5	4.2	0.5
	2	41.0	20.0	26.0	14.0
	3	158.0	138.0	127.0	119.0
CF-15-01	1	4.6	1.1	3.2	0.9
	2	32.5	14.0	20.0	9.0
	3	90.0	80.0	55.0	46.0
	4	240.0	235.0	140.0	133.0

536